

Supporting information

High-temperature energy storage performances of "isomer-like" polyimide and its thermoplastic polyurethane blending system

Xue-Jie Liu,^a Ming-Sheng Zheng,^{*a} Qingguo Chi,^b Yiyi Zhang,^c Zhi-Min Dang,^d

George Chen^e and Jun-Wei Zha ^{*a,f}

^a School of Chemistry and Biological Engineering, University of Science & Technology Beijing, Beijing 100083, P. R. China. E-mail: zhajw@ustb.edu.cn, zhengms@ustb.edu.cn

^b Key Laboratory of Engineering Dielectrics and Its Application, Harbin University of Science and Technology, Haerbin 150080, P. R. China

^c School of Electrical Engineering, Guangxi University, Nanning 530004, P. R. China

^d State Key Laboratory of Power System, Department of Electrical Engineering, Tsinghua University, Beijing 100084, P. R. China.

^e Department of Electronics and Computer Science, University of Southampton, Southampton SO17 1BJ, United Kingdom.

^f Shunde Graduate School of University of Science and Technology Beijing, Shunde 528399, P. R. China

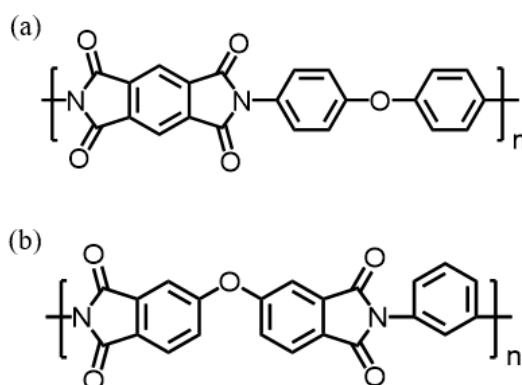


Fig. S1 Repeating unit structure of (a) common PI and (b) i-PI film.

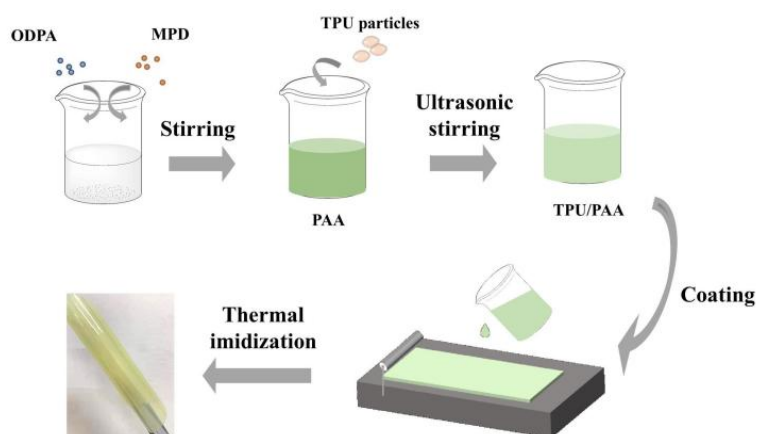


Fig. S2 Preparation process of the TPU/i-PI films.

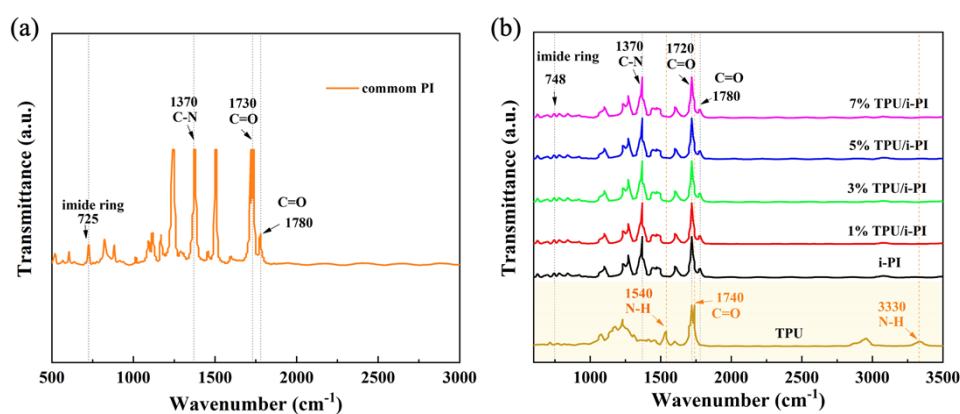


Fig. S3 FT-IR spectra of (a) common PI and (b) TPU, i-PI and TPU/i-PI films.

The characteristic imide absorption peaks of asymmetrical C=O stretching, symmetrical C=O stretching, C–N stretching and C=O bending of imide ring in common PI films are observed at 1780 cm^{-1} , 1720 cm^{-1} , 1370 cm^{-1} and 725 cm^{-1} respectively. The absorption peaks at 780 cm^{-1} , 1720 cm^{-1} , 1370 cm^{-1} and 748 cm^{-1} are associated with asymmetrical C=O stretching, symmetrical C=O stretching, C–N stretching and C=O bending of imide ring in i-PI film. The characteristic absorption peaks of N-H bending, C=O stretching and N-H stretching in TPU film are observed at 1540 cm^{-1} , 1740 cm^{-1} and 3330 cm^{-1} .

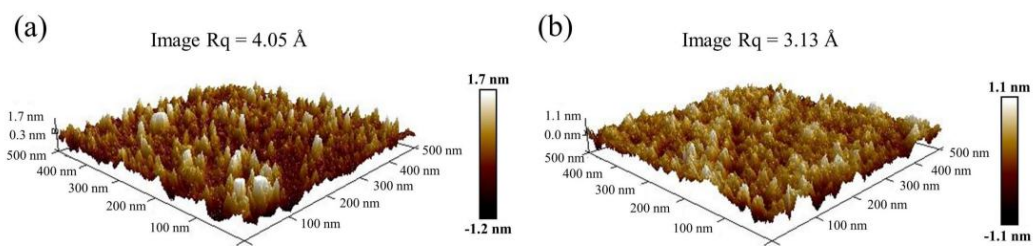


Fig. S4 AFM images of (a) i-PI and (b) 3% TPU/i-PI film.

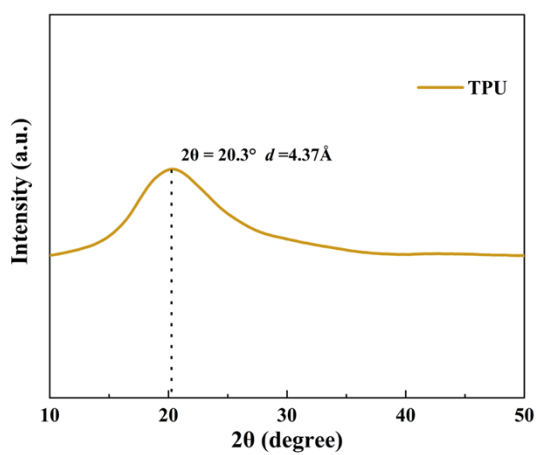


Fig. S5 XRD pattern of TPU film.

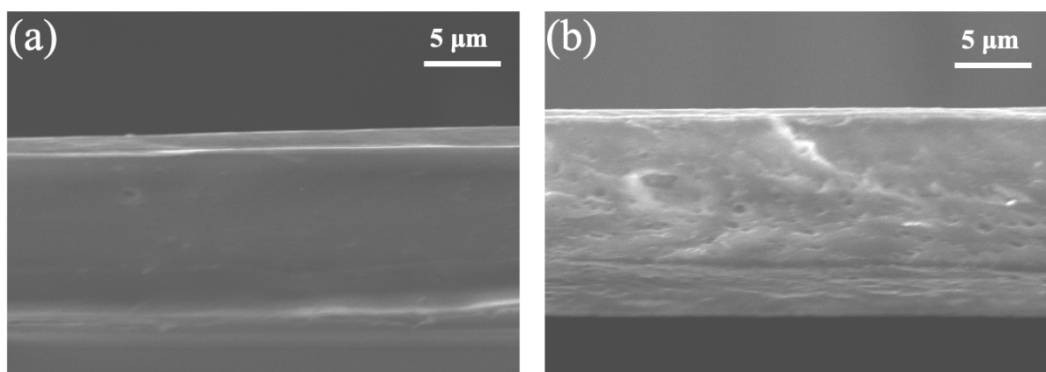


Fig. S6 SEM images of (a) 1% and (b) 7% TPU/i-PI film.

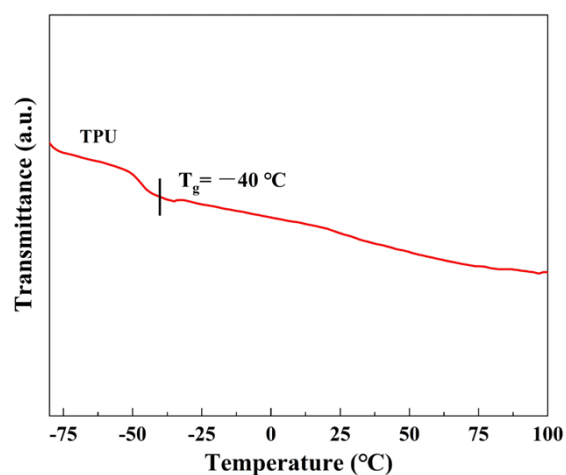


Fig. S7 DSC curve of TPU film.

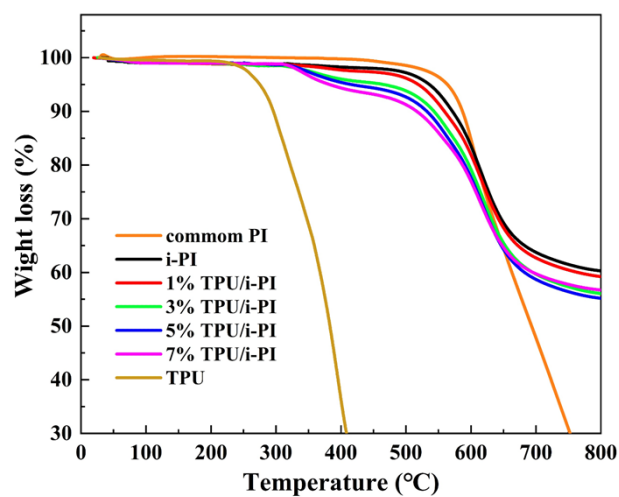


Fig. S8 TGA curves of TPU, common PI, i-PI and TPU/i-PI films.

Table S1 Thermal stability of TPU, common PI, i-PI and TPU/i-PI films.

Film	TPU	Common PI	i-PI	1% TPU/i-PI	3% TPU/i-PI	5% TPU/i-PI	7% TPU/i-PI
T_g (°C)	-40	302	257	257	254	256	256
$T_{d5\%}$ (°C)	275	563	536	518	465	416	382

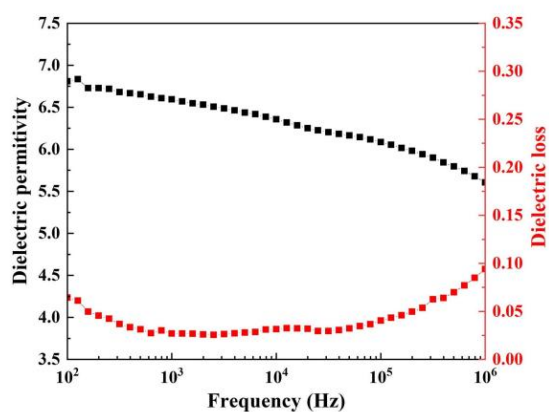


Fig. S9 Dielectric permittivity and loss of TPU film.

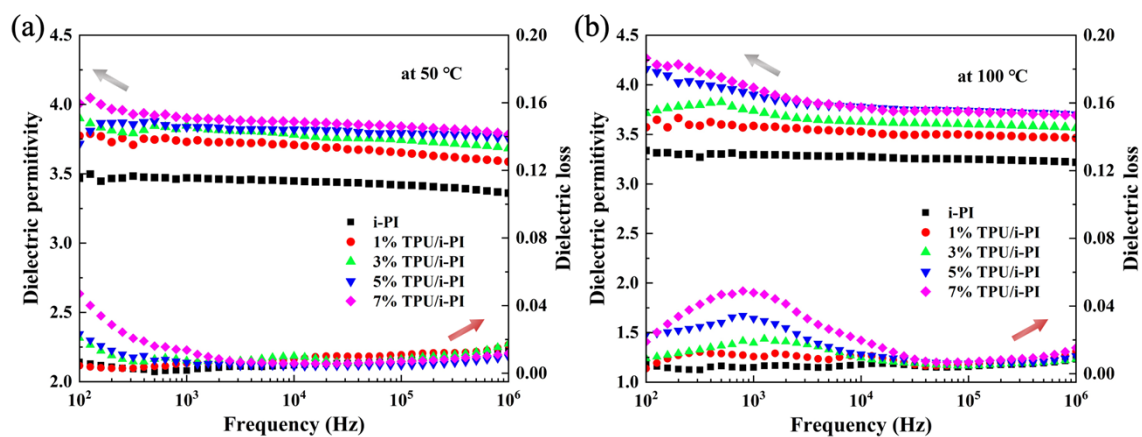


Fig. S10 Dielectric permittivity and loss of i-PI and TPU/i-PI films at (a) 50 °C and (b) 100 °C.

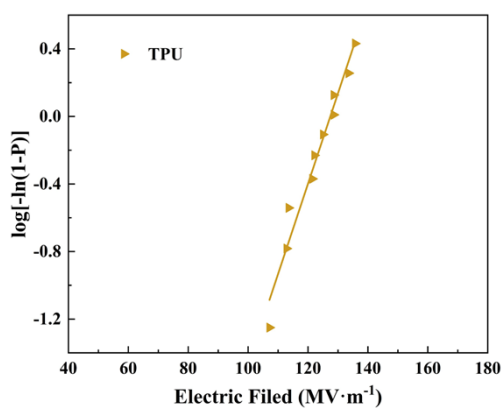


Fig. S11 Breakdown strength of TPU film.

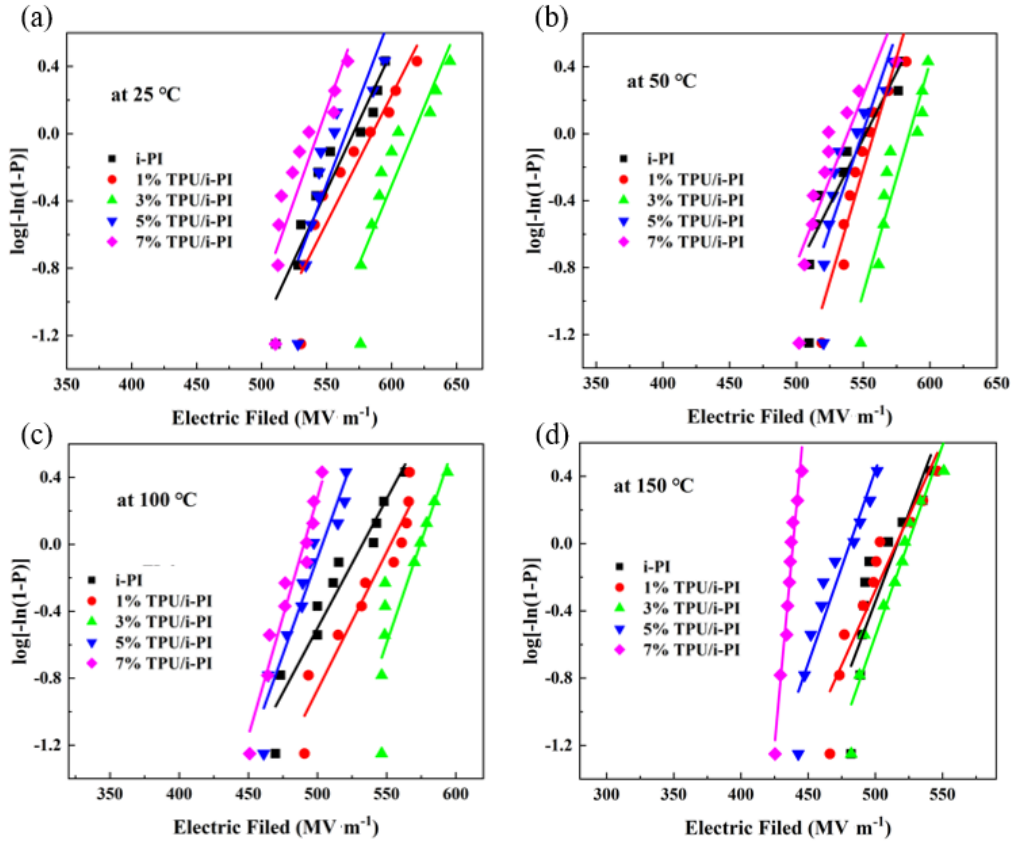


Fig. S12 Breakdown strength of i-PI and TPU/i-PI films at (a) 25 °C, (b) 50 °C, (c) 100 °C and (d) 150 °C.

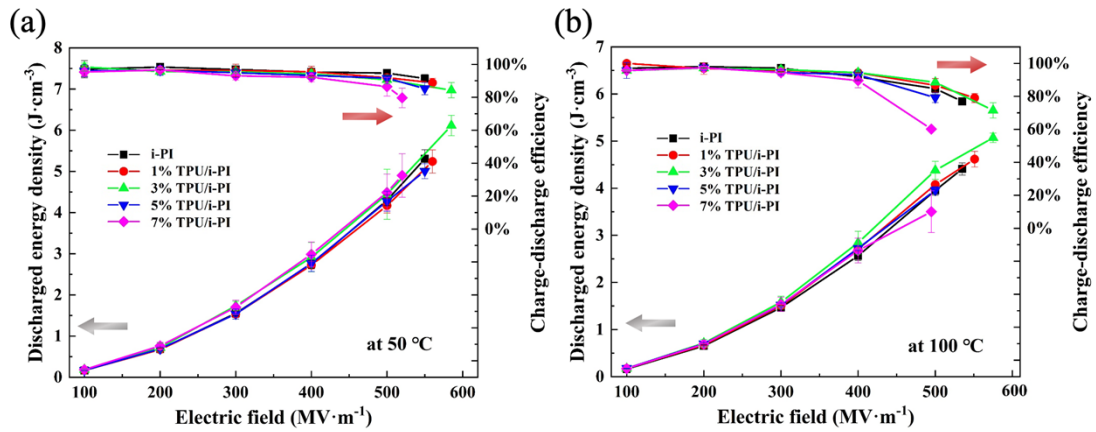


Fig. S13 The U_e and η of i-PI and TPU/i-PI films at (a) 50 °C and (b) 100 °C. The error bars are the standard deviation obtained from at least three measurements of the films.

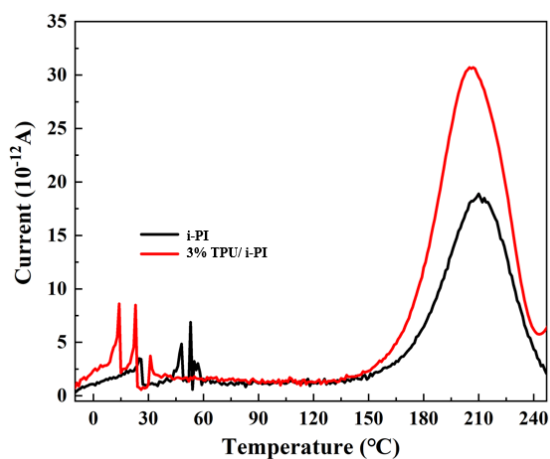


Fig. S14 TSDC curves of i-PI and 3% TPU/i-PI film.

Table S2. TSDC results and calculated trap energy level and trapped charges density of i-PI and 3% TPU/i-PI film.

Materials	Peak temperature (°C)	Peak current (10 ⁻¹² A)	Trap energy level (eV)	Trapped charge density (10 ¹⁸ eV ⁻¹ m ⁻³)
i-PI	210	1.89	1.20	3.93
3% TPU/i-PI	207	3.07	1.195	7.44

Bipolar carrier transport model

The bipolar charge transport model is established based on Poisson equation, current continuity equation, conduction equation, etc., which can simulate the migration, trapping, detrapping and recombination of electrons and holes in dielectrics.^[1] The specific formula refers to our previous work.^[2]

Table S3. Parameter settings for the bipolar carrier transport model

parameters	i-PI	3% TPU/i-PI
$B_{e, h}$	0.1 S^{-1}	0.1 S^{-1}
$n_{0\text{et}, \text{ht}}$	$3.93 \times 10^{18} \text{ eV}^{-1} \text{ m}^{-3}$	$7.44 \times 10^{18} \text{ eV}^{-1} \text{ m}^{-3}$
$\omega_{\text{et}, \text{ht}}$	1.203 eV	1.195 eV
S_0, S_1, S_2	$6.4 \times 10^{-22} \text{ m}^2 \text{ C}^{-1} \text{ s}^{-1}$	$6.4 \times 10^{-22} \text{ m}^2 \text{ C}^{-1} \text{ s}^{-1}$
S_3	$0 \text{ m}^2 \text{ C}^{-1} \text{ s}^{-1}$	$0 \text{ m}^2 \text{ C}^{-1} \text{ s}^{-1}$
$\omega_{\text{ci}, \text{hi}}$	1.2 eV	1.2 eV
E	50 MV m^{-1}	50 MV m^{-1}
ϵ_r	3.55	3.87
T	298 K	298 K

- [1] Y.Y. Zhang, G. Wang, X.T. Zhang, W.B. Zhong, Z.C. Su, C.Q. Xu, R.N. Wang, X.Y. Mao and J.F. Liu, *IEEE T. Plasma. Sci.*, 2022, **50**, 731-739.
- [2] X. J. Liu, M. S. Zheng, G. Wang, Y. Y. Zhang, Z. M. Dang, G. Chen and J. W. Zha, *J. Mater. Chem. A*, 2022, **10**, 10950-10959.